DOI: 10.1002/ejic.201001044

# Structural and Electronic Characteristics of a Novel BEDT-TTF Derivative: $[BEDT\text{-}TTF]_2[Cu_2Br_3]$

Frauke Schödel,[a] Ulrich Tutsch,[b] Friedhelm Isselbächer,[b] Dieter Schweitzer,[c] Inge Sänger,[a] Michael Bolte,[a] Jan W. Bats,[d] Jens Müller,[b] Michael Lang,[b] Matthias Wagner,[a] and Hans-Wolfram Lerner*[a]

**Keywords:** Conducting materials / Semiconductors / Copper / Bromine / Tetrathiafulvalene / Electrochemistry / Oxidation

Crystals of κ-$[(BEDT\text{-}TTF)_2][Cu(N(CN)_2)Br]$ were available with good quality and high reproducibility from the BEDT-TTF electro-oxidation with an electrolyte molar ratio $[Ph_4P][N(CN)_2]$:CuBr of 1:1 in a mixture of THF and ethylene glycol. Surprisingly, by varying the electrolyte molar ratio from 1:1 to 1:8 a novel type of BEDT-TTF salt, $[BEDT\text{-}TTF]_2[Cu_2Br_3]$, was formed. The solid-state structure of $[BEDT\text{-}TTF]_2[Cu_2Br_3]$ consists of stacks of non-coordinated BEDT-TTF molecules and stacks of the contact ions $[BEDT\text{-}TTF][Cu_2Br_3]$ (triclinic space group, *P*1). The two crystallographically independent $[BEDT\text{-}TTF][Cu_2Br_3]$ contact ions in the second stack are related by a pseudo-inversion center. Resistivity measurements on single crystals reveal that $[BEDT\text{-}TTF]_2[Cu_2Br_3]$ possesses a semiconductor-like behavior under normal pressure from room temperature down to at least 10 K.

## Introduction

Bis(ethylenedithio)tetrathiafulvalene (BEDT-TTF) derivatives have gained prominence in wide areas of research.[1–6] Since 1990, the conductivity of BEDT-TTF salts, especially those with the formula $[(BEDT\text{-}TTF)_2][Cu(N(CN)_2)X]$ (X = Cl, Br, I, $Br_{1-x}I_x$, $Br_{1-x}Cl_x$), has been extensively studied. It has been shown that this family of isostructural compounds exhibits a wide diversity of electronic properties ranging from insulating to semiconducting and "bad metallic" to superconducting behavior, which strongly depend on the hydrostatic pressure, see, for example, ref.[7] for a review. Recent studies revealed that the compounds $[(BEDT\text{-}TTF)_2][Cu(N(CN)_2)X]$ (X = Br, $Br_{0.5}Cl_{0.5}$, $Br_{0.7}Cl_{0.3}$) undergo a transition to a superconducting state with $T_c$ = 11.4–11.6 K at ambient pressure,[1,8] whereas $[(BEDT\text{-}TTF)_2][Cu(N(CN)_2)X]$ (X = Cl, I, $Br_{0.9}I_{0.1}$) are insulators[2,9] at low temperatures. For the latter, superconductivity can be induced by the application of moderate pressure in the kbar range.[1,9,10] Due to the relationship between structure and electronic properties, the solid-state structures of BEDT-TTF salts are of great interest. Generally, the compounds $[(BEDT\text{-}TTF)_2][Cu(N(CN)_2)X]$ (X = Cl, Br, I, $Br_{1-x}I_x$, $Br_{1-x}Cl_x$) are prepared by electro-oxidation of BEDT-TTF in organic solvents on a Pt anode under galvanostatic conditions. Normally, a mixed electrolyte containing $[N(CN)_2]^-$ and CuX is used. Investigations of BEDT-TTF electro-oxidation in the presence of these electrolytes revealed that the composition of the anion subsystem in the resulting salts, and therefore the solid-state structure, depends on the nature of the counterion of $[N(CN)_2]^-$ and on the solvent used. In this paper, we report a modified procedure to prepare single crystals of κ-$[(BEDT\text{-}TTF)_2][Cu(N(CN)_2)Br]$ by BEDT-TTF electro-oxidation using a mixed electrolyte, in which $[Ph_4P][N(CN)_2]$ and CuBr in a 1:1 molar ratio have been weighed in for the starting composition. We stress, however, that the exact amount of dissolved CuBr has not been determined. When the same procedure was followed varying the electrolyte molar ratio $[Ph_4P][N(CN)_2]$:CuBr from 1:1 to 1:8, a novel type of BEDT-TTF salt, $[BEDT\text{-}TTF]_2[Cu_2Br_3]$ was formed. Here we report the solid-state structure and the resistivity of $[BEDT\text{-}TTF]_2[Cu_2Br_3]$.

## Results and Discussion

### Syntheses

In the literature, a successful electro-oxidation of BEDT-TTF has been reported for the synthesis of κ-$[(BEDT\text{-}TTF)_2][Cu(N(CN)_2)Br]$.[1–6,11] In this present

---

[a] Institut für Anorganische Chemie, Goethe-Universität,
Frankfurt am Main, Max-von-Laue-Straße 7, 60438 Frankfurt am Main, Germany
Fax: +49-69/79829260
E-mail: lerner@chemie.uni-frankfurt.de
[b] Physikalisches Institut, Goethe-Universität,
Frankfurt am Main, Max-von-Laue-Straße 1, 60438 Frankfurt am Main, Germany
[c] Physikalisches Institut, Universität Stuttgart,
Pfaffenwaldring 57, 70550 Stuttgart, Germany
[d] Institut für Organische Chemie, Goethe-Universität,
Frankfurt am Main, Max-von-Laue-Straße 7, 60438 Frankfurt am Main, Germany

Supporting information for this article is available on the WWW under http://dx.doi.org/10.1002/ejic.201001044.

study, we report a modified procedure to prepare single crystals of κ-[(BEDT-TTF)$_2$][Cu(N(CN)$_2$)Br] by BEDT-TTF electro-oxidation using a mixed electrolyte with the starting composition of [Ph$_4$P][N(CN)$_2$] and CuBr in a 1:1 molar ratio. Crystals synthesized along this route[12] are characterized by high superconducting transition temperatures, narrow 10–90% transition widths, low residual resistivities, and high residual resistivity ratios. All these quantities reflect the materials' high crystalline perfection and a low defect concentration.

When a solution of BEDT-TTF in a mixture of THF and ethylene glycol was placed in a three-chamber electrochemical cell, single crystals of κ-[(BEDT-TTF)$_2$]-[Cu(N(CN)$_2$)Br] (**1**) were grown at a constant voltage of 1.30 V, corresponding to a current between 14.3 and 47.0 µA. Crystals of mm size grew after a period of 6–12 d (Figure 1). The BEDT-TTF salt **1** was obtained with good quality and high reproducibility. Derivative **1** was characterized by X-ray structure analysis.[13]

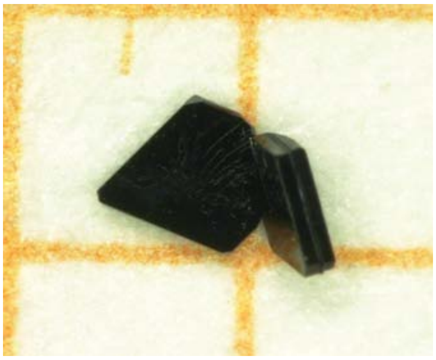

Figure 1. Crystals of κ-[(BEDT-TTF)$_2$]Cu[N(CN)$_2$]Br (**1**) obtained by the electro-oxidation of BEDT-TTF with the molar electrolyte ratio [Ph$_4$P][N(CN)$_2$]:CuBr of 1:1.

Surprisingly, when the procedure was followed under the same conditions, but with the electrolyte molar ratio [Ph$_4$P][N(CN)$_2$]:CuBr of 4:7 instead of 1:1, crystals of [BEDT-TTF]$_2$[Cu$_2$Br$_3$] (**2**) along with those of known BEDT-TTF derivative **1** were found (Scheme 1; Figure 2). Moreover, when the electro-oxidation was performed with the electrolyte molar ratio of 1:8, the BEDT-TTF salt **2** was formed exclusively. In contrast to BEDT-TTF electro-oxidation, the chemical oxidation of BEDT-TTF with [Me$_4$N]$_2$[CuBr$_4$] yields [BEDT-TTF][Cu$_2$Br$_3$].[14] Based on this evidence, the presence of [Ph$_4$P][N(CN)$_2$] and its concentration relative to that of CuBr are apparently essential for the formation of **2**. The crystal-determining step for **2** is probably not the conversion of the BEDT-TTF molecule into its cation, but appears to be a pre-orientation of BEDT-TTF molecules by the anion of the electrolyte during the BEDT-TTF oxidation.

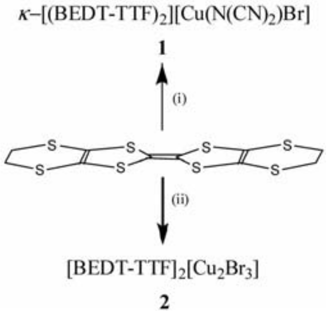

Scheme 1. Electro-oxidation of BEDT-TTF with the electrolyte molar ratio [Ph$_4$P][N(CN)$_2$]:CuBr of 1:1 (i) and 1:8 (ii).

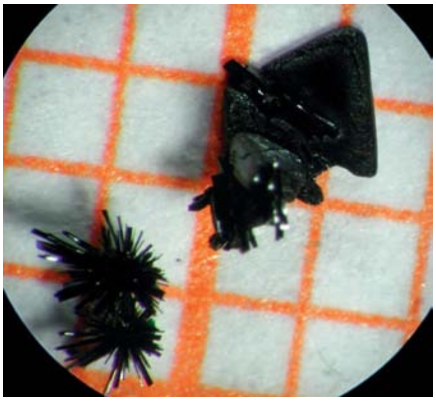

Figure 2. Crystals of κ-[(BEDT-TTF)$_2$]Cu[N(CN)$_2$]Br (**1,** plates) and [BEDT-TTF]$_2$[Cu$_2$Br$_3$] (**2**, needles) obtained by the electro-oxidation of BEDT-TTF with the molar electrolyte ratio [Ph$_4$P][N(CN)$_2$]:CuBr of 4:7.

## Structure of [BEDT-TTF]$_2$[Cu$_2$Br$_3$] (2)

Figure 3 represents the solid-state structure of **2** (triclinic, *P*1); the selected bond lengths and angles are listed in the figure caption and additional data are given in Table 1. The unit cell of the crystal structure of **2** contains two independent formula units. The solid-state structure of **2** consists of a stack of non-coordinated BEDT-TTF molecules and a second stack of two crystallographic independent contact ions of [BEDT-TTF][Cu$_2$Br$_3$]. These contact ions in **2** are related by a pseudo-inversion center.

As shown in Figure 4, the anions [Cu$_2$Br$_3$]$^-$ in **2** form infinite chains along the *a*-direction. A similar structure motif for the [Cu$_2$Br$_3$]$^-$ anion has been found in the solid-state structure of the related complexes [BEDT-TTF]-[Cu$_2$Br$_3$][14] and [BEDT-TTF]$_3$[Cu$_2$Br$_3$]$_2$.[15] The Cu atoms in **2** have a distorted tetrahedral coordination and are bound by three Br atoms and a S atom of a BEDT-TTF group. The Cu atoms in **2** that are bridged by two Br atoms show the rather short Cu···Cu interatomic distances of 2.713(7) Å [for Cu(1)–Cu(2)] and 2.737(7) Å [for Cu(3)–Cu(4)]. The Cu atoms, which are bridged by Cu–BEDT-TTF or Cu–Br units, feature very long Cu···Cu interatomic distances (4.063 and 4.038 Å, respectively). Similar chains, but with the slightly longer Cu···Cu distance of 2.931 Å have been observed in the crystal structure of [BEDT-TTF][Cu$_2$Br$_3$] and [BEDT-TTF]$_2$[Cu$_2$Br$_3$]$_2$(BEDT-TTF). In the structure of [BEDT-TTF][Cu$_2$Br$_3$] and [BEDT-TTF]$_2$-[Cu$_2$Br$_3$]$_2$(BEDT-TTF) as well as in **2**, [Cu$_2$Br$_3$]$^-$ anions have been found in which all Cu atoms are in the +1 oxi-

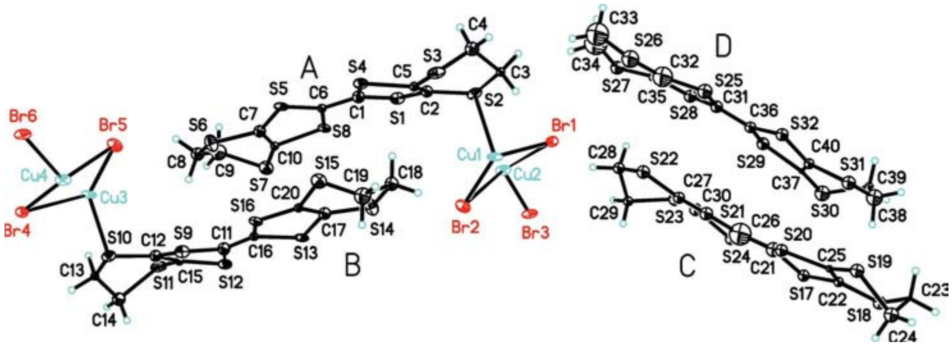

Figure 3. Structure of [BEDT-TTF]$_2$[Cu$_2$Br$_3$] (**2**) in the crystal; displacement ellipsoids are drawn at the 50% probability level. Selected bond lengths [Å] and angles [°]: Br(1)–Cu(2) 2.511(7), Br(3)–Cu(2) 2.464(7), Br(3)–Cu(1)#1 2.465(7), Br(2)–Cu(1) 2.428(7), Br(2)–Cu(2) 2.479(7), Cu(2)–S(3)#1 2.360(13), Cu(2)···Cu(1) 2.713(7), Cu(1)–S(2) 2.391(13), Cu(1)–Br(3)#2 2.465(7), S(5)–C(6) 1.59(3), S(5)–C(7) 1.73(4), S(1)–C(1) 1.74(4), S(1)–C(2) 1.85(4), S(6)–C(8) 1.68(4), S(6)–C(7) 1.80(4), S(2)–C(3) 1.77(3), S(2)–C(2) 1.79(4), S(3)–C(4) 1.66(4), S(3)–C(5) 1.67(4), S(3)–Cu(2)#2 2.360(13), S(7)–C(10) 1.63(3), S(7)–C(9) 1.86(4) S(4)–C(1) 1.69(4), S(4)–C(5) 1.87(4), S(8)–C(6) 1.88(3), S(8)–C(10) 1.94(3), C(10)–C(7) 1.31(5), C(2)–C(5) 1.28(5), C(6)–C(1) 1.46(5), C(3)–C(4) 1.68(5), C(8)–C(9) 1.37(5) Br(4)–Cu(3) 2.535(7), Br(4)–Cu(4) 2.541(7), Br(6)–Cu(4) 2.410(7), Br(6)–Cu(3)#2 2.425(7), Br(5)–Cu(4) 2.435(7), Br(5)–Cu(3) 2.443(7), Cu(4)–S(11)#2 2.333(13), Cu(4)···Cu(3) 2.737(7), Cu(3)–S(10) 2.339(12), Cu(3)–Br(6)#1 2.425(7), S(13)–C(17) 1.69(4), S(13)–C(16) 1.90(4), S(9)–C(11) 1.62(4), S(9)–C(12) 1.68(4), S(14)–C(17) 1.72(4), S(14)–C(18) 1.92(4), S(10)–C(12) 1.68(4), S(10)–C(13) 1.85(3), S(11)–C(15) 1.83(4), S(11)–C(14) 1.96(4), S(11)–Cu(4)#1 2.333(13), S(15)–C(19) 1.60(4), S(15)–C(20) 1.83(3), S(12)–C(15) 1.70(4), S(12)–C(11) 1.90(4), S(16)–C(20) 1.58(3), S(16)–C(16) 1.62(3), C(20)–C(17) 1.52(5), C(12)–C(15) 1.46(5), C(16)–C(11) 1.35(5), C(13)–C(14) 1.46(5), C(18)–C(19) 1.73(6), S(20)–C(21) 1.55(4), S(20)–C(25) 1.77(4), S(19)–C(25) 1.65(4), S(19)–C(24) 1.97(4), S(18)–C(22) 1.75(3), S(18)–C(23) 1.81(3), C(25)–C(22) 1.33(4), S(24)–C(26) 1.67(5), S(24)–C(30) 1.71(4), S(23)–C(30) 1.78(4), S(23)–C(29) 1.87(3), S(22)–C(27) 1.66(4), S(22)–C(28) 1.88(4), C(27)–C(30) 1.42(5), C(27)–S(21) 1.84(4), S(17)–C(21) 1.82(4), S(17)–C(22) 1.89(3), S(21)–C(26) 1.74(5), C(28)–C(29) 1.62(4), C(21)–C(26) 1.53(6), S(25)–C(32) 1.66(6), S(25)–C(31) 1.69(4), S(27)–C(34) 1.68(6), S(27)–C(35) 1.74(4), S(26)–C(32) 1.69(6), S(26)–C(33) 1.77(5), S(31)–C(39) 1.73(4), S(31)–C(40) 1.79(4), S(30)–C(37) 1.66(3), S(30)–C(38) 1.87(3), S(28)–C(31) 1.68(4), S(28)–C(35) 1.87(4), S(32)–C(36) 1.74(3), S(32)–C(40) 1.75(3), C(32)–C(35) 1.45(6), C(40)–C(37) 1.31(4), S(29)–C(36) 1.71(3), S(29)–C(37) 1.84(3), C(38)–C(39) 1.31(5), C(36)–C(31) 1.46(4), C(23)–C(24) 1.50(5), C(34)–C(33) 1.39(7), Cu(1)–Br(1)–Cu(2) 65.8(2), Cu(2)–Br(3)–Cu(1)#1 111.1(2), S(3)#1–Cu(2)–Br(3) 123.8(4), S(3)#1–Cu(2)–Br(2) 110.2(4), Br(3)–Cu(2)–Br(2) 105.0(2), S(3)#1–Cu(2)–Br(1) 99.7(4), Br(3)–Cu(2)–Br(1) 109.9(3), Br(2)–Cu(2)–Br(1) 107.4(2), S(2)–Cu(1)–Br(2) 122.5(4), S(2)–Cu(1)–Br(3)#2 109.6(4), Br(2)–Cu(1)–Br(3)#2 104.6(3), S(2)–Cu(1)–Br(1) 91.4(4), Br(2)–Cu(1)–Br(1) 109.8(3), Br(3)#2–Cu(1)–Br(1) 119.7(3), S(11)#2–Cu(4)–Br(6) 121.4(4), S(11)#2–Cu(4)–Br(5) 108.9(4), Br(6)–Cu(4)–Br(5) 108.8(3), S(11)#2–Cu(4)–Br(4) 97.7(4), Br(6)–Cu(4)–Br(4) 109.9(3), Br(5)–Cu(4)–Br(4) 109.4(3), S(10)–Cu(3)–Br(6)#1 107.3(4), S(10)–Cu(3)–Br(5) 122.5(4), Br(6)#1–Cu(3)–Br(5) 105.9(3), S(10)–Cu(3)–Br(4) 91.8(4), Br(6)#1–Cu(3)–Br(4) 120.6(3), Br(5)–Cu(3)–Br(4) 109.4(2), S(10)–Cu(3)–Cu(4) 102.9(4). Symmetry transformations used to generate equivalent atoms: #1: *x* – 1, *y*, *z*; #2: *x* + 1, *y*, *z*.

Table 1. Crystallographic data and further details of the structure determination of **2** and [Ph$_4$P][N(CN)$_2$].

| | **2** | [Ph$_4$P][N(CN)$_2$] |
|---|---|---|
| Empirical formula | $C_{20}H_{16}Br_3Cu_2S_{16}$ | $C_{26}H_{20}N_3P$ |
| Color | brown | colorless |
| Formula weight | 1136.10 | 405.42 |
| Crystal system | triclinic | tetragonal |
| Space group | *P*1 | *I*41/*a* |
| *a* [Å] | 6.7649(2) | 17.0494(9) |
| *b* [Å] | 7.7725(2) | 17.0494(9) |
| *c* [Å] | 31.9377(2) | 7.5243(5) |
| *α* [deg] | 84.8500(10) | 90 |
| *β* [deg] | 86.1410(10) | 90 |
| *γ* [deg] | 89.1300(10) | 90 |
| Volume [Å$^3$], *Z* | 1668.65(7) | 2187.2(2) |
| Density (calcd.) [Mg/m$^3$] | 2.261 | 1.231 |
| Absorption coefficient, $\mu$(Mo-$K_\alpha$) [mm$^{-1}$] | 5.886 | 0.143 |
| *F*(000) | 1110 | 848 |
| Crystal size [mm] | 0.55 × 0.12 × 0.04 | 0.35 × 0.34 × 0.33 |
| Diffractometer | Siemens CCD | Stoe-IPDS-II |
| $\theta$ range [deg] | 1.92–27.00 | 3.80–25.00 |
| Index ranges | $-8 \le h \le 8$,<br>$-9 \le k \le 9$,<br>$-39 \le l \le 40$ | $-19 \le h \le 20$,<br>$-20 \le k \le 20$,<br>$-8 \le l \le 8$ |
| Number of reflections collected | 22336 | 18568 |
| Number of independent reflections | 12693 | 956 |
| *R*(int) | 0.1272 | 0.0760 |
| Absorption correction | semi-empirical from equivalents | semi-empirical from equivalents |
| Number of data/ restraints/parameter | 12693/3/371 | 956/0/76 |
| Goodness of fit on $F^2$ | 1.183 | 1.232 |
| Final *R* indices [$I > 2\sigma(I)$], *R*1, *wR*2 | 0.1345, 0.3071 | 0.0941, 0.2226 |
| Largest diff. peak/hole [e Å$^{-3}$] | 2.327/–2.300 | 0.382/–0.251 |

dation state.[16,17] It has been shown that copper(II) halides readily oxidize neutral BEDT-TTF molecules. Kanehama et al. used the reaction between BEDT-TTF and $CuBr_2$ to synthesize the [BEDT-TTF] salts with $Cu^{II}$-containing anions ([BEDT-TTF][$Cu_2Br_4$], [BEDT-TTF]$_2$[$Cu_6Br_{10}$], [BEDT-TTF]$_2$[$Cu_3Br_7$]), and [BEDT-TTF]$_2$[$Cu_2Br_3$]$_2$-(BEDT-TTF), as well as [BEDT-TTF]$_2$[$Cu_2Br_4$] in which the Cu atoms of the anions are in the +1 oxidation state.[15] In the Cambridge Crystallographic Database, structures of neutral BEDT-TTF molecules cannot be found together with $Cu^{II}$ ions in one crystal. Due to the difference in their redox potentials, neutral BEDT-TTF molecules do not exist in the presence of $Cu^{II}$ ions. Additionally, measurements in a SQUID magnetometer have been performed that reveal the absence of paramagnetic moments resulting from $Cu^{II}$ ions in single crystals of **2**.[18] In the structure of **2**, short Cu–S bond distances have been found between the BEDT-TTF moiety and the [$Cu_2Br_3$]$^-$ anions of the contact ion pair. As shown in Figures 5 and 6, the BEDT-TTF stacking pattern in **2** differs significantly from those of **1** (Figure 7) and [(BEDT-TTF)][$Cu_2Br_3$]. In detail, the BEDT-TTF units in **2** form two different types of stacks in the *b*-direction: (i) stacks of noncoordinated BEDT-TTF molecules and (ii) stacks of the contact ion pairs [BEDT-TTF][$Cu_2Br_3$]. Contrary to **2**, the structure of **1** displays only one type of stack; these are built by singly charged pairs (dimers) of BEDT-TTF molecules. As mentioned above, in [BEDT-TTF][$Cu_2Br_3$] only contact ion pairs of [BEDT-TTF]$^+$ cations and [$Cu_2Br_3$]$^-$ anions are found. It should be noted that the stacking pattern observed in **2** has not been found in any other BEDT-TTF complex. The BEDT-TTF molecules as well as the [BEDT-TTF]$^+$ cations in **2** are non-planar and are considerably bent. The outer six-membered rings of the BEDT-TTF molecules, as well as those of the [BEDT-TTF]$^+$ cations, have envelope or twist

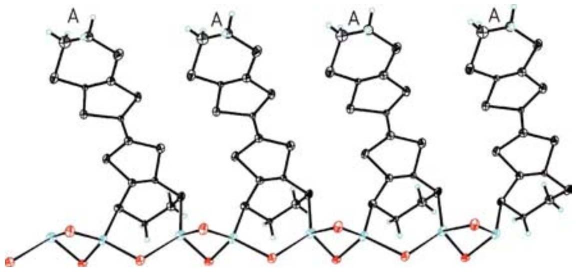

Figure 4. Connectivity of the polymeric anion [$Cu_2Br_3$]$^-$ in [BEDT-TTF]$_2$[$Cu_2Br_3$] (**2**).

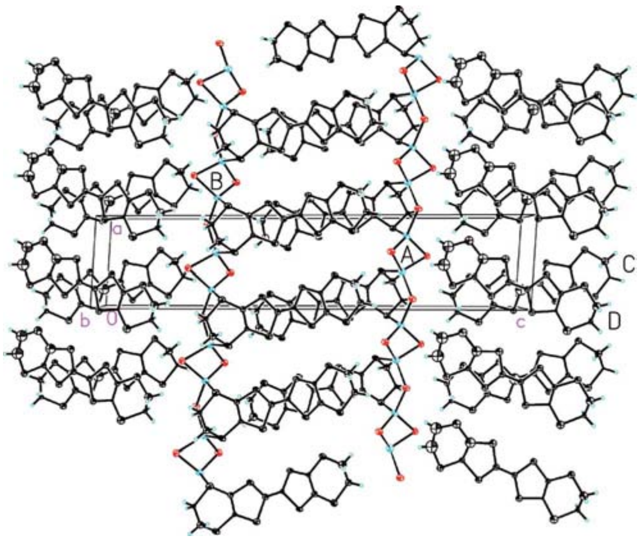

Figure 6. Crystal packing diagram of [BEDT-TTF]$_2$[$Cu_2Br_3$] (**2**) along the *b*-axis.

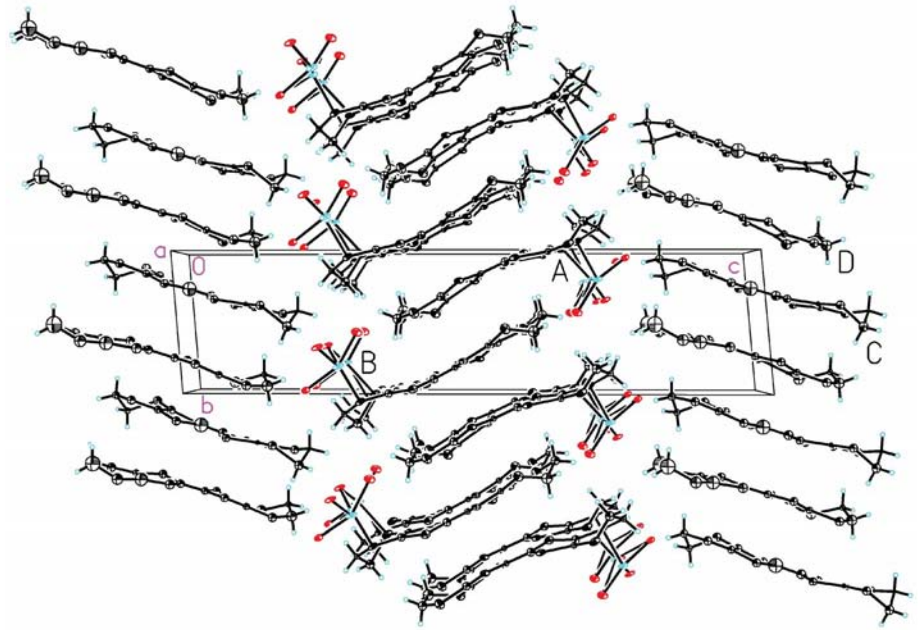

Figure 5. Crystal packing diagram of [BEDT-TTF]$_2$[$Cu_2Br_3$] (**2**) along the *a*-axis.

conformations. The distance between the central carbon atoms of the BEDT-TTF units can be used as a diagnostic test for the determination of charge occupation in BEDT-TTF molecules.[19] The values of the central C–C bond lengths of the BEDT-TTF units in **2** are between 1.35(5) and 1.53(6) Å (average value: 1.45 Å). Apparently these bond lengths lie more in the range expected for [BEDT-TTF]$^+$ cations than that for neutral BEDT-TTF molecules (C=C bond length in BEDT-TTF: 1.32 Å). The crystal packing diagram of **2** reveals seven intermolecular CH···Br contacts with the H···Br interatomic distances between 2.68 and 2.91 Å.

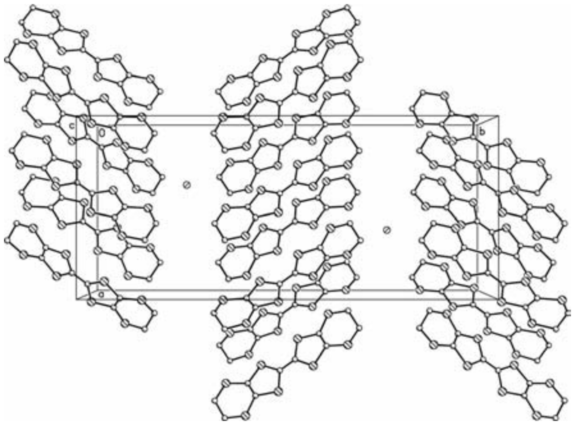

Figure 7. Stacking pattern of [BEDT-TTF]$_2$ dimers in κ-[(BEDT-TTF)$_2$]Cu[N(CN)$_2$]Br (**1**) along the *c*-axis.

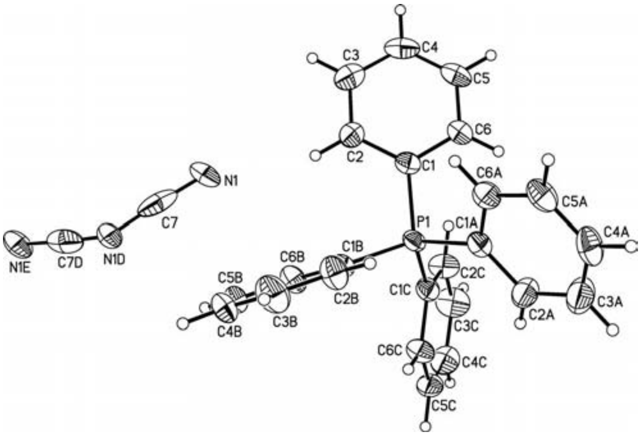

Figure 8. Structure of [Ph$_4$P][N(CN)$_2$] in the crystal; displacement ellipsoids are drawn at the 50% probability level. Selected bond lengths [Å] and angles [°]: Selected bond lengths [Å] and angles [°]: P(1)–C(1)#2 1.800(5), P(1)–C(1) 1.800(5), P(1)–C(1)#3 1.800(5), C(1)–C(6) 1.397(6), C(1)–C(2) 1.396(7), C(2)–C(3) 1.401(7), C(4)–C(5) 1.366(8), C(5)–C(6) 1.386(7), C(7)–N(1) 1.335(17), C(7)–N(1) #4 1.373(17), N(1)–C(7)#5 1.373(17), C(1)#1-P(1)–C(1)#2 110.52(15), C(1)#1-P(1)–C(1) 107.4(3), C(1)#2-P(1)–C(1) 110.52(15), C(1)#1–P(1)–C(1)#3 110.52(15), C(1)#2-P(1)–C(1)#3 107.4(3), C(1)–P(1)–C(1)#3 110.52(15), C(6)–C(1)–C(2) 119.8(4), C(6)–C(1)–P(1) 119.1(4), C(2)–C(1)–P(1) 121.1(4), C(1)–C(2)–C(3) 119.4(5), C(4)–C(3)–C(2) 119.5(5), C(5)–C(4)–C(3) 121.1(5), C(4)–C(5)–C(6) 119.9(5), C(5)–C(6)–C(1) 120.4(5), N(1)–C(7)–N(1)#4 175.3(10), C(7)–N(1)–C(7)#5 115.5(8). Symmetry transformations used to generate equivalent atoms: #1: $-x + 1$, $-y + 3/2$, $z + 0$; #2: $-y + 5/4$, $x + 1/4$, $-z + 5/4$; #3: $y - 1/4$, $-x + 5/4$, $-z + 5/4$; #4: $-y + 7/4$, $x + 1/4$, $z + 1/4$; #5: $y - 1/4$, $-x + 7/4$, $z - 1/4$.

## Structure of [Ph$_4$P][N(CN)$_2$]

X-ray quality crystals of [Ph$_4$P][N(CN)$_2$] were obtained from recrystallization with ethanol. The phosphonium dicyanamide [Ph$_4$P][N(CN)$_2$] crystallizes in the tetragonal space group $I4_1/a$. The P···N interatomic distance of 5.273 Å between the center of the cation in [Ph$_4$P]$^+$ and the center of the anion in [N(CN)$_2$]$^-$ is significantly longer than the sum of the atomic radii. As depicted in Figure 8, the NC–N–CN skeleton of the dicyanamide anion is not linear [C–N–C = 115.5(8)°; N–C–N = 175.3(10)°]. The structure of the anion [N(CN)$_2$]$^-$ reveals CN bond lengths between 1.335(17) and 1.373(17) Å, which lie between a CN double and a CN triple bond. The P atom of the phosphonium cation in [Ph$_4$P][N(CN)$_2$] has an ideal tetrahedral coordination and is bound to four phenyl rings. The structural parameters found in [Ph$_4$P][N(CN)$_2$] are in the expected range. Data on the structure collection is given in Table 1.

## Resistivity of [BEDT-TTF]$_2$[Cu$_2$Br$_3$]

Four-probe measurements of the resistivity $\rho$ (current along the *a*-axis) on a crystal of **2** have been performed with an ac resistance bridge (Linear Research Inc., model LR-700) from room temperature (293 K) down to 10 K. To extend the accessible resistance range (maximal 2 MΩ for the LR-700), a parallel resistor of 1.8 MΩ was used, which enabled us to measure resistances up to 200 MΩ.

The resistivity, shown in Figure 9, has a negative temperature derivative over the whole temperature range. Such behavior is typical for semiconductors in which electrical transport is due to the excitation of electrons from the valence band to the conduction band or for materials in which electrical transport occurs by electron hopping. For a semiconductor, the resistivity should be well described (at least

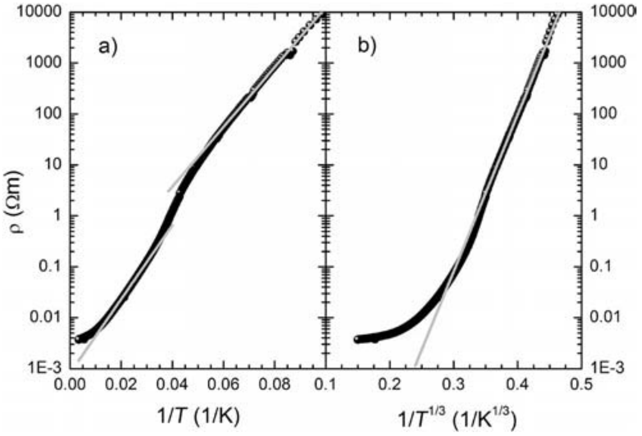

Figure 9. Temperature dependence of the resistivity along the *a*-axis of [BEDT-TTF]$_2$[Cu$_2$Br$_3$] in a representation log(T) versus $1/T$ (a) and $\log(T)$ versus $1/T^{1/3}$ (b).

at high temperatures) by $\rho = A \exp[\Delta/(2k_BT)]$, in which $\Delta$ is the energy gap, resulting in a straight line in a $\log(T)$ versus $1/T$ representation. As shown in Figure 9a, such behavior describes the data reasonably well over the whole temperature range investigated. More precisely, there are two temperature ranges, $T < 17$ K and $35\text{ K} < T < 65$ K, in which a semiconductor-like behavior is very well obeyed, with corresponding gap values of $\Delta_1$ = 23 meV and $\Delta_2$ = 29 meV, respectively. Introducing a temperature-dependent gap $\Delta(T)$ would improve the fit but leaves the average gap size unaffected.

In the case of hopping conductivity (variable range hopping), the resistivity should vary as $\rho = B \exp[(T_0/T)^{1/(1+d)}]$, with an exponent of $(1 + d)^{-1} = 1/3$ for a quasi 2D ($d = 2$) system, which, according to the crystal structure, is likely to apply to the present material. As shown in Figure 9b, the resistivity data are well described by this formula for temperatures $T < 23$ K. At higher temperatures, however, the data deviate significantly from the expectation for a hopping conductivity.

From the resistivity data alone, no conclusion can be made with respect to the mechanism of electrical transport, except that it is thermally activated. Although the semiconductor model provides a better overall description, the variable-range hopping model is superior at low temperatures ($T < 23$ K). Resistivity measurements under pressure might help to distinguish between the two models as one would expect the band gap and the hopping probability to behave quantitatively differently when pressure is changed.

## Conclusion

In summary, it has been shown that crystals of **1** were available with good quality and high reproducibility by BEDT-TTF electro-oxidation with the electrolyte molar ratio $[Ph_4P][N(CN)_2]$:CuBr of 1:1 in a mixture of THF and ethylene glycol. Surprisingly, when the same procedure was followed using the electrolyte molar ratio $[Ph_4P][N(CN)_2]$:CuBr of 1:8, crystals of a novel type of BEDT-TTF salt, $[BEDT\text{-}TTF]_2[Cu_2Br_3]$, were obtained. The presence of $[Ph_4P][N(CN)_2]$ and its concentration relative to that of CuBr is apparently essential for the formation of **2**. The crystal-determining step for **2** is probably not the conversion of the BEDT-TTF molecule into its cation, but appears to be a pre-orientation of BEDT-TTF molecules by the anion of the electrolyte during the BEDT-TTF oxidation. The solid-state structure of **2** differs significantly from those of **1** and $[BEDT\text{-}TTF][Cu_2Br_3]$. In derivative **2**, stacks of non-coordinated BEDT-TTF molecules, as well as stacks of the contact ion pairs $[BEDT\text{-}TTF][Cu_2Br_3]$ are found, whereas the structure of $[BEDT\text{-}TTF][Cu_2Br_3]$ features only $[BEDT\text{-}TTF][Cu_2Br_3]$ contact ion pairs and the structure of **1** displays stacks consisting of positively charged pairs of BEDT-TTF molecules. Resistivity measurements of single crystals reveal that $[BEDT\text{-}TTF]_2[Cu_2Br_3]$ possesses a semiconductor-like behavior under normal pressure from room temperature down to at least 10 K.

## Experimental Section

**General Remarks:** The BEDT-TTF electro-oxidation was carried out under dry argon ($O_2$ value < 1 ppm and $H_2O$ value < 1 ppm). THF was distilled from sodium/benzophenone and ethylene glycol from Mg under an argon atmosphere prior to use. BEDT-TTF, $[Ph_4P]Cl$, and CuBr were purchased from commercial sources. BEDT-TTF and $[Ph_4P]Cl$ were purified prior to use by repeated recrystallization. X-ray crystallographic data of $[Ph_4P]Cl$ are listed in the Supporting Information. CuBr was recrystallized several times from dry THF under an argon atmosphere in the glove box. The NMR spectra were recorded on a Bruker AM 250, a Bruker DPX 250, a Bruker Avance 300, and a Bruker Avance 400 spectrometer. Abbreviations: d = doublet; *i* = *ipso*; *o* = *ortho*; *m* = *meta*, *p* = *para*; mult = multiplet; br. = broad.

**Synthesis of $[Ph_4P][N(CN)_2]$:** The phosphonium dicyanamide $[Ph_4P][N(CN)_2]$ was prepared from precursor $[Ph_4P]Cl$ and $K[N(CN)_2]$ according to a literature procedure.[20] When $[Ph_4P]Cl$ was treated with $K[N(CN)_2]$, $[Ph_4P][N(CN)_2]$ was formed in good yield. $[Ph_4P][N(CN)_2]$ was purified by multiple recrystallization from ethanol. Selected data for $[Ph_4P][N(CN)_2]$: thermal decomposition 210 °C. $^1H$ NMR ($CD_3OD$, internal TMS): $\delta$ = 7.77 (mult; 4 H Ph), 7.96 (mult; 1 H Ph) ppm. $^{13}C\{^1H\}$NMR ($CD_3OD$, internal TMS): $\delta$ = 119.5 (d; $^1J_{PC}$ = 89.71 Hz, *i*-Ph), 120.5 [br.; N-$(CN)_2$], 131.7 (d; $^2J_{PC}$ = 12.93 Hz, *o*-Ph), 135.9 (d; $^3J_{PC}$ = 89.71 Hz, *m*-Ph), 136.7 (d; $^4J_{PC}$ = 3.0 Hz, *p*-Ph) ppm. $^{31}P\{^1H\}$NMR ($CDCl_3$, external TMS): $\delta$ = 23.2 ($Ph_4P^+$) ppm. $C_{26}H_{20}N_3P$ (405.43): calcd. C 77.02, H 4.97, N 10.36; found C 77.04, H 4.93, N 10.43.

**Synthesis of κ-$[(BEDT\text{-}TTF)_2][Cu(N(CN)_2)Br]$ (1):** The single crystals of κ-$[(BEDT\text{-}TTF)_2][Cu(N(CN)_2)Br]$ were prepared by the electro-oxidation of BEDT-TTF (60 mg, 0.16 mmol) in THF (90 mL) and ethylene glycol (20 mL) on a Pt anode under galvanostatic regime at 20.5–20.8 °C. An electrolyte containing $[Ph_4P][N(CN)_2]$ (253 mg, 0.62 mmol) and CuBr (81 mg, 0.56 mmol) in a 1:1 molar ratio was used. A voltage of 1.29 V was applied between the electrodes for the crystal growth. This resulted in a current density at the electrodes of 18.8 μA/cm² at the beginning and 5.7 μA/cm² at the end of the growth procedure. The crystals of κ-$[(BEDT\text{-}TTF)_2][Cu(N(CN)_2)Br]$ were grown on the anode after 6 d (Figure 1). The product **1** was identified by X-ray single crystal and X-ray powder diffraction.[13] Selected data for **1**: MS-MALDI: *m*/*z* (%) = 384 (100) $[BEDT\text{-}TTF]^+$. $C_{20}H_{16}Br_3Cu_2S_{16}$ (1136.19): calcd. C 26.99, H 1.65, N 4.29; found C 26.86, H 1.60, N 4.30.

**Synthesis of $[BEDT\text{-}TTF]_2[Cu_2Br_3]$ (2):** Crystals of $[BEDT\text{-}TTF]_2[Cu_2Br_3]$ were grown by electro-oxidation of BEDT-TTF (60 mg, 0.16 mmol) in a mixture of THF (90 mL) and ethylene glycol (20 mL) on a Pt anode under galvanostatic regime at 20.5–20.8 °C. The electrolyte containing $[Ph_4P][N(CN)_2]$ (63 mg, 0.16 mmol) and CuBr (182 mg, 1.26 mmol) was dissolved. A voltage of 1.29 V was applied between the electrodes for the crystal growth. This resulted in a current density at the electrodes of 7.6 μA/cm² at the beginning and 2.5 μA/cm² at the end of the growth procedure. The crystals of **2** appeared on the anode as needles after 6 d. Selected data for **2**: IR (KBr): $\tilde{\nu}$ = 1410 [s, ν(CC)], 1387 (m), 1267 (s), 1117 (m), 1044 (w), 1013 (m), 990 (w), 882 (w) cm⁻¹. MS-MALDI: *m*/*z* (%) = 384 (100) $[BEDT\text{-}TTF]^+$. $C_{20}H_{16}Br_3Cu_2S_{16}$ (1136.19): calcd. C 21.14, H 1.42; found C 21.02, H 1.29.

**Remark:** Single crystals of $[BEDT\text{-}TTF]_2[Cu_2Br_3]$ (**2**) were grown simultaneously with crystals of the known κ-$[(BEDT\text{-}TTF)_2][Cu(N(CN)_2)Br]$ (**1**) by electro-oxidation of BEDT-TTF (60 mg, 0.16 mmol) in a mixture of THF (90 mL) and ethylene glycol

(20 mL) on a Pt anode under a galvanostatic regime at 21.5–23.0 °C. The electrolyte containing $[\mathrm{Ph_4P}][\mathrm{N(CN)_2}]$ (85 mg, 0.21 mmol) and CuBr (50 mg, 0.35 mmol) was dissolved. A current of 8.5 μA in the beginning and 4.0 μA at the end and a constant voltage of 1.3 V were applied for the crystals' growth. The crystals of **2** (45%) appeared on the anode as needles along with **1** (55%) after 32 d (Figure 2). The products **1** and **2** were identified by X-ray single crystal and X-ray powder diffraction.

**X-ray Crystallographic Study:** Data collection: Stoe-IPDS-II diffractometer and Siemens CCD three-circle diffractometer, empirical absorption correction using MULABS[21] and SADABS,[22] structure solution by direct methods,[23] structure refinement: full-matrix least-squares on $F^2$ with SHELXL-97.[24] Hydrogen atoms were placed on ideal positions and refined with fixed isotropic displacement parameters using a riding model.

CCDC-748974 (for **1**), -785384 (for **2**), -748972 (for $[\mathrm{Ph_4P}][\mathrm{N(CN)_2}]$), and -748973 (for $[\mathrm{Ph_4P}]\mathrm{Cl}$) contain the supplementary crystallographic data for this paper. These data can be obtained free of charge from The Cambridge Crystallographic Data Centre via www.ccdc.cam.ac.uk/data_request/cif.

**Supporting Information** (see footnote on the first page of this article): Crystallographic characterization of $[\mathrm{Ph_4P}]\mathrm{Cl}$.

## Acknowledgments

Financial support by the Deutsche Forschungsgemeinschaft (DFG) (SFB/TRR 49) is gratefully acknowledged.

---

[1] A. M. Kini, U. Geiser, H. H. Wang, K. D. Carlson, J. M. Williams, W. K. Kwok, K. G. Vandervoort, J. E. Thompson, D. L. Stupka, D. Jung, M.-H. Whangbo, *Inorg. Chem.* **1990**, *29*, 2555–2557.

[2] J. M. Williams, A. M. Kini, H. H. Wang, K. D. Carlson, U. Geiser, L. K. Montgomery, G. J. Pyrka, D. M. Watkins, J. M. Kommers, S. J. Boryschuk, A. V. S. Crouch, W. K. Kwok, J. E. Schirber, D. L. Overmyer, D. Jung, M.-H. Whangbo, *Inorg. Chem.* **1990**, *29*, 3272–3274.

[3] H. Yamochi, T. Komatsu, N. Matsukawa, G. Saito, T. Mori, M. Kusunoki, K. Sakaguchi, *J. Am. Chem. Soc.* **1993**, *115*, 11319–11327.

[4] H. Urayama, H. Yamochi, G. Saito, S. Sato, A. Kawamoto, J. Tanaka, T. Mori, Y. Maruyama, H. Inokuchi, *Chem. Lett.* **1988**, 463–466.

[5] U. Geiser, M. A. Beno, A. M. Kini, H. H. Wang, A. J. Schultz, B. D. Gates, C. S. Cariss, K. D. Carlson, J. M. Williams, *Synth. Met.* **1988**, *27*, A235–A241.

[6] U. Geiser, A. M. Kini, H. H. Wang, M. A. Beno, J. M. Williams, *Acta Crysallogr., Sect. C* **1991**, *47*, 190–192.

[7] N. Toyota, M. Lang, J. Müller, *Low-Dimensional Molecular Metals*, Springer Series in Solid-State Sciences, vol. 154, Springer, Berlin, **2007**.

[8] N. D. Kushch, L. I. Buravov, A. G. Khomenko, E. B. Yagubskii, L. P. Rosenberg, R. P. Shibaeva, *Synth. Met.* **1993**, *53*, 155–160; N. D. Kushch, A. V. Kazakova, L. I. Buravov, A. N. Chekhlov, A. D. Dubrovskii, E. B. Yagubskii, E. Canadell, *J. Solid State Chem.* **2009**, *182*, 617–621.

[9] H. H. Wang, K. D. Carlson, U. Geiser, A. M. Kini, A. J. Schultz, J. M. Williams, L. K. Montgomery, W. K. Kwok, U. Welp, K. G. Vandervoort, S. J. Boryschk, A. V. Strieby Crouch, J. M. Kommers, D. M. Watkins, J. E. Schirber, D. L. Overmyer, D. Jung, J. J. Novoa, M.-H. Whangboo, *Synth. Met.* **1991**, *42*, 1983–1990; N. D. Kushch, L. I. Buravov, A. G. Khomenko, S. I. Pesotskii, V. N. Laukhin, E. B. Yagubskii, R. P. Shibaeva, V. E. Zavodnik, L. P. Rozenberg, *Synth. Met.* **1995**, *72*, 181–184; Yu. V. Sushko, V. A. Bondarenko, R. A. Petrosov, N. D. Kusch, E. B. Yagubskii, *Phys. C* **1991**, *185*, 2683–2684.

[10] M. A. Tanatar, S. Kagoshima, T. Ishiguro, H. Ito, V. S. Yafanov, V. A. Bondarenko, N. D. Kushch, E. B. Yagubskii, *Phys. Rev. B* **2000**, *62*, 15561–15568.

[11] Y. Watanabe, H. Sato, T. Sasaki, N. Toyota, *J. Phys. Soc. Jpn.* **1991**, *60*, 3608–3611.

[12] C. Strack, C. Akinci, V. Pashenko, B. Wolf, E. Uhrig, W. Assmus, M. Lang, J. Scheurer, L. Wiehl, J. A. Schlueter, J. Wosnitza, D. Schweitzer, J. Müller, J. Wykhoff, *Phys. Rev. B* **2005**, *72*, 054511-1-054511-10.

[13] Structural details: CCDC-748974.

[14] M. B. Inoue, M. Inoue, M. A. Brucka, Q. Fernando, *J. Chem. Soc., Chem. Commun.* **1993**, 515–516.

[15] R. Kanehama, M. Umemiya, F. Iwahori, H. Miyasaka, K. Sugiura, M. Yamashita, Y. Yokochi, H. Ito, S. Kuroda, H. Kishida, H. Okamoto, *Inorg. Chem.* **2003**, *42*, 7173–7181.

[16] Examples for mixed-valence polymeric $\mathrm{Cu^ICu^{II}}$-containing anions: $[\mathrm{Cu^I_4Cu^{II}_2Br_{10}}]^2$, $[\mathrm{Cu^ICu^{II}_2Br_7}]^{2-}$, $[\mathrm{Cu^ICu^{II}Br_4}]^-$; see ref.[15,17]

[17] Cambridge Structural Database (CSD, version 5.29 with three updates, January **2008**); F. H. Allen, *Acta Crystallogr., Sect. B* **2002**, *58*, 380; G. Margraf, M. Bolte, M. Wagner, H.-W. Lerner, *J. Chem. Crystallogr.* **2007**, *37*, 503–506.

[18] Magnetization measurements have been performed by using a SQUID magnetometer for a 1.24 mg sample (composed of several single crystals) between 2 and 290 K in a magnetic field of $B = 4.5$ T. A very small paramagnetic signal was found. By assigning this signal to the magnetization of localized (quasi-) free spin ($S$) entities, their concentration can be determined by fitting the data with an expression for the Langevin paramagnetism, i.e., $M(T) = N/V \mu_B g/2\,\{(2S + 1)\coth[(2S + 1)\,x] - \coth(x)\}$, $x = g\mu_B{\cdot}B/(2k_BT)$. By using $g = 2$, $S = 1/2$, appropriate for $\mathrm{Cu^{II}}$ centers, we find a density of $N/V = 0.012$ $\mathrm{Cu^{II}}$ ions per unit cell, corresponding to 0.003 $\mathrm{Cu^{II}}$ ions per Cu site. This is consistent with the regular Cu ions being in an oxidation state $\mathrm{Cu^+}$ ($S = 0$) and a small amount of $S = 1/2$ impurities.

[19] P. Guionneau, C. J. Kepert, G. Bravic, D. Chasseau, M. R. Truter, M. Kurmoo, P. Day, *Synth. Met.* **1997**, *86*, 1973–1974; M. A. Beno, U. Geiser, A. M. Kini, H.-H. Wang, K. D. Carlson, M. M. Miller, T. J. Allen, J. A. Schlueter, R. B. Proksch, J. M. Williams, *Synth. Met.* **1988**, *27*, A209–A217.

[20] H. Köhler, T. P. Lischko, H. Hartung, A. M. Golub, *Z. Anorg. Allg. Chem.* **1974**, *403*, 35–40.

[21] R. H. Blessing, *Acta Crystallogr., Sect. A* **1995**, *51*, 33.

[22] G. M. Sheldrick, *SADABS*, University of Göttingen, Germany, **2000**.

[23] G. M. Sheldrick, *Acta Crystallogr. A* **1990**, *46*, 467.

[24] G. M. Sheldrick, *SHELXL-97*, *A Program for the Refinement of Crystal Structures*, University of Göttingen, Germany, **1997**.

Received: October 1, 2010